Electrocatalytic Dioxygen Reduction on Underpotentially Deposited Tl on Au(111) Studied by an Active Site Blocking Strategy

Ilwhan Oh,[†] Andrew A. Gewirth,*[,‡] and Juhyoun Kwak*[,†]

Department of Chemistry, Korea Advanced Institute of Science and Technology (KAIST), 373-1 Kusong-dong Yusong-gu, Taejon 305-701, Korea, and Department of Chemistry and the Frederick Seitz Materials Research Laboratory, University of Illinois, Urbana, Illinois 61801

Received January 23, 2001

Electrochemical measurements and in situ scanning tunneling microscopy (STM) are performed to establish a structure−reactivity correlation for peroxide or dioxygen reduction on underpotentially deposited (upd) Tl on Au(111) in 0.1 M $HClO_4$. At the potential of catalytic activity toward the O_2 reduction, STM reveals the presence of Tl islands on the Au(111) terrace with height of 0.24 ± 0.03 nm. These islands expand in size and number, as the potential becomes more negative, but the full Tl monolayer formed at −0.2 V vs NHE is catalytically inactive. Ethanethiol (EtSH) significantly inhibits the H_2O_2 reduction, and the kinetics and thermodynamics of EtSH adsorption on the Tl upd are quantitatively analyzed. STM shows that EtSH introduction leads to the formation of a 0.15 nm high terrace along the edges of the Tl islands. This terrace is assigned to EtSH bound to the Au surface near the Tl islands with the alkyl chain oriented roughly perpendicular to the surface. These results show that edge sites around the Tl island are the active site of catalytic O_2 reduction by Tl upd on Au(111).

1. Introduction

Relating surface structure to its chemical reactivity is a necessary step in developing an understanding of electrode reactivity and is considered one of the most important themes in surface chemistry.[1] In the electrochemical environment, such efforts have been quite challenging,[2−4] partly due to the limited number of in situ experimental tools that can provide structural information of the electrode surface at atomic level. Development of in situ techniques such as scanning probe microscopes (SPM)[5] and surface X-ray scattering (SXS)[6] has revolutionized the field of surface electrochemistry by providing detailed information on the electrode surface processes such as reconstruction, etching, and adsorption.

Dioxygen reduction on the electrode surface is one of the most fundamental electrochemical reactions. This reaction is relevant to processes occurring not only in fuel cell systems but also to those related to corrosion and metal−air batteries. Consequently, dioxygen reduction has been well-studied.[4,7] O_2 reduction on different electrodes is believed to proceed via a H_2O_2 intermediate

$$O_2 + 2H^+ + 2e^- \rightarrow H_2O_2 \quad (1)$$

$$H_2O_2 + 2H^+ + 2e^- \rightarrow 2H_2O \quad (2)$$

in which the $2e^-$ reduction of H_2O_2 in eq 2 is often the limiting step in the O_2 reduction scheme. However, there is little direct evidence concerning the mode of association of the dioxygen molecule with any surface.

One way to examine mechanisms of dioxygen or peroxide electroreduction is through recourse to catalysts made utilizing the underpotential deposition (upd) process.[4,8] There are several upd metals including Bi, Pb, and Tl on Au(111), which are known to catalyze the electroreduction of O_2.[9] While the structure of Bi[10,11] and Pb[14−18] in the catalytically active region is known, the structure of Tl upd on Au(111) in the acid electrochemical environment is still unclear. In the alkaline environment, both STM[19] and SXS[20] studies showed that a close-packed rotated hexagonal structure exists prior to bulk deposition and that a low-coverage structure at positive potentials was associated with catalytic activity toward the O_2 reduction. In the acid environment, SXS studies[21] revealed a rotated

* Corresponding authors. J. Kwak: fax, +82-42-869-2810; e-mail: jhkwak@cais.kaist.ac.kr. A. A. Gewirth: fax, +1-217-333-8329; e-mail, agewirth@uiuc.edu.

[†] Korea Advanced Institute of Science and Technology.

[‡] University of Illinois at Urbana-Champaign.

(1) Whitesides, G. *Angew. Chem., Int. Ed. Engl.* **1990**, *29*, 1209−1218.
(2) Sun, S.-G. In *Electrocatalysis*; Lipkowski, J., Ross, P. N., Eds.; Wiley-VCH: New York, 1998.
(3) Jarvi, T. D.; Stuve, E. M. In *Electrocatalysis*; Lipkowski, J., Ross, P. N., Eds.; Wiley-VCH: New York, 1998; pp 75−154.
(4) Adzic, R. In *Electrocatalysis*; Lipkowski, J., Ross, P. N., Eds.; Wiley-VCH: New York, 1998; pp 197−242.
(5) Gewirth, A. A.; Niece, B. K. *Chem. Rev.* **1997**, *97*, 1129−1162.
(6) Robinson, I. K. *Rep. Prog. Phys.* **1992**, *55*, 599−651.
(7) Tarasevich, M. R.; Sadkowski, A.; Yeager, E. In *Oxygen Electrochemistry*; Conway, B. E., Bockris, J. O. M., Yeager, E., Kahn, S. U. M., White, R. E., Eds.; Plenum: New York, 1983; Vol. 7, pp 301−398.
(8) Kolb, D. M. In Advances in *Electrochemistry and Electrochemical Engineering*; Gerischer, H., Tobias, C. W., Eds.; Wiley: New York, 1978; Vol. 11, pp 125−271.
(9) Sayed, S. M.; Juttner, K. *Electrochim. Acta* **1983**, *28*, 1635−1641.
(10) Chen, C.-H.; Gewirth, A. A. *J. Am. Chem. Soc.* **1992**, *114*, 5439.
(11) Chen, C.-h.; Kepler, K. D.; Gewirth, A. A.; Ocko, B. M.; Wang, J. *J. Phys. Chem.* 1993, **97**, 7290−7294.
(12) Carnal, D.; Oden, P. I.; Mueller, U.; Schmidt, E.; Siegenthaler, H. *Electrochim. Acta* **1995**, *40*, 1223−1235.
(13) Sackmann, J.; Bunk, A.; Potzschke, R. T.; Staikov, G.; Lorenz, W. J. *Electrochim. Acta* **1998**, *43*, 2863−2873.
(14) Green, M. P.; Hanson, K. J.; Scherson, D. A.; Xing, X.; Richter, M.; Ross, P. N.; Carr, R.; Lindau, I. *J. Phys. Chem.* **1989**, *93*, 2181−2189.
(15) Green, M. P.; Hanson, K. J.; Carr, R.; Lindau, I. *J. Electrochem. Soc.* **1990**, *137*, 3493−3498.
(16) Binggeli, M.; Carnal, D.; Nyffengger, R.; Siegenthaler, H.; Christoph, R.; Roher, H. *J. Vac. Sci. Technol., B* **1991**, *9*, 1985−1992.
(17) Green, M. P.; Hanson, K. J. *Surf. Sci. Lett.* **1991**, *259*, L743.
(18) Tao, N. J.; Pan, J.; Li, Y.; Oden, P. I.; DeRose, J. A.; Lindsay, S. M. *Surf. Sci.* **1992**, *271*, L338−344.
(19) Polewska, W.; Wang, J. X.; Ocko, B. M.; Adzic, R. R. *J. Electroanal. Chem.* **1994**, *376*, 41−47.
(20) Wang, J. X.; Adzic, R. R.; Ocko, B. M. *J. Phys. Chem.* **1994**, *98*, 7182−7190.
(21) Adzic, R. R.; Wang, J. X.; Ocko, B. M. *Electrochim. Acta* **1995**, *40*, 83−89.

10.1021/la010297u CCC: $20.00
Published on Web 05/11/2001

hexagonal Tl adlayer in the negative potential region, while no X-ray scattering intensity was observed at positive potentials, in the catalytically active region. On the basis of their voltammetric similarities, we proposed that the adlayer structures of Pb and Tl upd on Au(111) would resemble each other,[22] as will be verified in this work.

There are competing theories concerning the mechanism of electrocatalytic O_2 reduction in upd systems. For Bi upd on Au(111),[23] an AFM study showed that the O_2 reduction is catalyzed only in the specific potential region where an open (2×2) Bi adlayer is present, in which both Bi and Au atoms are accessible to the adsorbing O_2 molecule. We postulated that the heterobimetallic site in the (2×2) Bi on Au(111) is the active site of catalysis. Likewise, for Pb upd on Au(111), both STM[14−18] and AFM[24] studies showed that, in the potential region of catalytic activity, the Pb adlayer exhibits an island structure on the Au(111) terrace. The island edge site, where both Pb and Au are available, was postulated to be the locus of catalytic activity. In both Bi[25] and Tl[22] upd on Au(111), it was revealed that a large amount of OH^- is coadsorbed, which must play roles in maintaining the open adlayer structure and in catalyzing the O_2 reduction.[22] The role of OH^- in the catalytic activity of the Au(100) surface was also recognized, in which the $4e^-$ reduction of O_2 occurs at the potential where the OH^- is adsorbed on the electrode.[26]

On the other hand, in a SXS study of TlBr on Au(111) in acid solution,[27] Adzic and Wang showed that the surface Tl coverage is reduced when O_2 reduction occurs. This suggests that a homogeneous mechanism invoking Tl oxidation followed by subsequent reduction and redeposition of Tl is responsible for O_2 reduction activity.

We have utilized a new strategy to search for the active site of upd electrocatalysis, in which a probe molecule is introduced onto the catalyst surface to block the active site.[28,29] The probe molecule/catalyst composite forms a static structure and provides a way to locate the active site on the catalyst surface. In one of the most successful examples of this strategy in ultrahigh vacuum, Over et al.[30] introduced CO as a probe molecule at low temperature on the RuO_2(110) surface. RuO_2 catalyzes CO oxidation. The adsorbed CO molecule, which could be imaged by STM because of its low mobility, is bonded to the coordinately unsaturated Ru atom, which was then assigned to the active site. The active site blocking strategy was also adapted in the electrochemical environment to locate the active site in the (2×2) Bi upd on Au(111).[28] When SCN^- was introduced into the (2×2) Bi on Au(111) as a poison, the surface IR spectroscopy showed that SCN^- was bound to the Au. This means that the lone Au site might be where O_2 binds in the catalytic reduction process.

In this paper, we use in situ STM to visualize the structure of the Tl upd adlayer developed on Au(111) in the acid electrochemical environment. This adlayer occurs in the potential region that exhibits electrocatalytic activity toward O_2 or peroxide reduction. We also use the active-site blocking strategy in order to further interrogate the electrocatalytic behavior.

2. Experimental Section

Electrochemical solutions were prepared from ultrapure water (Modulab, US Filter, MA, >18 MΩ) and $TlNO_3$ (Aldrich, 99.999%) with 0.1 M $HClO_4$ (Aldrich, double-distilled) as supporting electrolyte and ethanethiol (97%, Aldrich) as poison. The working electrode for cyclic voltammetric and chronoamperometric measurements was a Au(111) single crystal (MaTeck, Germany) with a diameter of 0.95 cm and a nominal area of 0.71 cm^2. The crystal was annealed for 3 min in a hydrogen flame prior to use and quenched in ultrapure water or slowly cooled in air. Oxide formation and stripping voltammetry of the surface in pure electrolyte was found to closely match the literature for Au(111).[31]

Voltammetric data were collected using a Pt wire counter electrode and a saturated Hg/Hg_2SO_4 reference electrode connected to the electrochemical cell via a capillary salt bridge to minimize contamination from the reference electrode. All potentials in this paper are reported relative to the normal hydrogen electrode (NHE). The solutions were purged with Ar prior to use, and an atmosphere of Ar was maintained in the cell during all electrochemical measurements. Potential control and sweeps were established using an Autolab potentiostat (Eco Chemie, Netherlands). Rotating disk electrode (RDE) measurements were obtained using a BAS model RDE-1 rotator (Bioanalytical Systems, IN) equipped with a collet, which holds the Au single crystal to form a hanging meniscus with electrolyte.

STM images were obtained in constant current mode with Topometrix TMX2000 which was calibrated against a highly ordered pyrolytic graphite (HOPG) surface in air for in-plane dimensions and against monatomic Au(111) steps for dimensions normal to the surface. An electrochemically etched Pt/Ir wire (Molecular Imaging, AR) coated with Apiezon wax or polyethylene was used as the STM tip.

The working electrode for STM imaging was Au evaporated onto glass (Metallhandel Schroer GmbH, Germany) or onto mica (Molecular Imaging) and annealed following a published procedure.[32] A gold/gold oxide or a Pt wire served as the reference electrode while a Pt wire was used for the counter electrode. Images were obtained in height mode and typically took 1 min to complete. All images are presented unfiltered.

3. Results and Analysis

3.1. Catalytic Reduction of H_2O_2 by Tl upd. Figure 1a shows a cyclic voltammogram obtained in 5 mM $TlNO_3$ and 0.1 M $HClO_4$ on a Au(111) single crystal. This voltammetry is identical with that previously reported.[21,22] A sharp cathodic peak C is observed at −0.19 V, and the corresponding anodic peak is split into two components, A_1 and A_2. Although no distinct voltammetric features are observed at potentials positive of peak A_2, chronocoulometric measurements revealed that the Au surface is covered with up to 0.55 monolayer of Tl in the positive potential region.[22]

Figure 1b shows voltammetry obtained in 10 mM H_2O_2 and 0.1 M $HClO_4$ on a Au(111) single crystal rotating at 400 rpm both with (solid line) and without (dashed line) the presence of 5 mM $TlNO_3$. This voltammetry is nearly identical with that previously reported.[21] In Figure 1b, the peroxide electroreduction current obtained in the presence of Tl begins to increase even at very positive potentials, where no distinct voltammetric features are observed in Figure 1a, and reaches its maximum at −0.33 V. The current then suddenly drops to a small value at

(22) Niece, B. K.; Gewirth, A. A. *J. Phys. Chem. B* **1998**, *102*, 818−823.
(23) Chen, C.-H.; Gewirth, A. A. *J. Am. Chem. Soc.* **1992**, *114*, 5439.
(24) Chen, C.-H.; Washburn, N.; Gewirth, A. A. *J. Phys. Chem.* **1993**, *97*, 9754−9760.
(25) Niece, B. K.; Gewirth, A. A. *Langmuir* **1996**, *12*, 4909−4913.
(26) Strbac, S.; Adzic, R. R. *J. Electroanal. Chem.* **1996**, *403*, 169−181.
(27) Adzic, R. R.; Wang, J. X. *J. Phys. Chem. B* **2000**, *104*, 869−872.
(28) Oh, I.; Biggin, M. E.; Gewirth, A. A. *Langmuir* **2000**, *16*, 1397−1406.
(29) Hsieh, S.-J.; Gewirth, A. A. *Langmuir* **2000**, *16*, 9501.
(30) Over, H.; Kim, Y. D.; Seitsonen, A. P.; Wendt, S.; Lundgren, E.; Schmid, M.; Varga, P.; Morgante, A.; Ertl, G. *Science* **2000**, *287*, 1474−1476.
(31) Angerstein-Kozlowska, H.; Conway, B. E.; Hamelin, A.; Stoicoviciu, L. *J. Electroanal. Chem.* **1987**, *228*, 429−453.
(32) Will, T.; Dietterle, M.; Kolb, D. M. In *Nanoscale Probes of the Solid−Liquid Interface*; Gewirth, A. A., Siegenthaler, H., Eds.; Kluwer: Dordrecht, The Netherlands, 1995; Vol. 228, p 137.

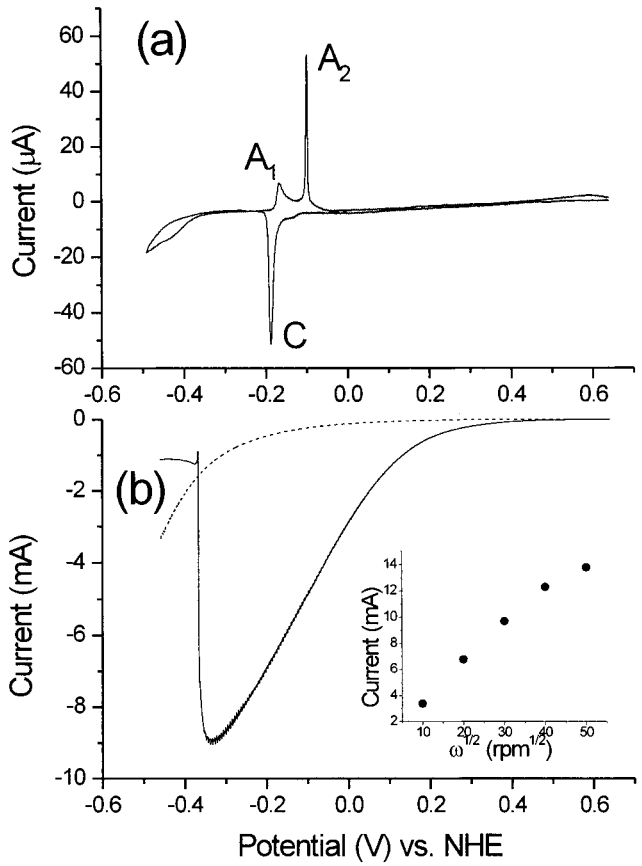

Figure 1. (A) CV in 5 mM $TlNO_3$ and 0.1 M $HClO_4$ on a Au(111) single crystal. Scan rate = 20 mV/s. (B) RDE voltammogram in 10 mM H_2O_2, 5 mM $TlNO_3$, and 0.1 M $HClO_4$. Rotation speed = 400 rpm. Scan rate = 20 mV/s. Dashed line: control experiment without Tl^+. Inset: plot of current as a function of rotation rate obtained at the maximum of electroreduction activity.

−0.37 V, indicating the occurrence of a dramatic change in the Tl upd adlayer. The chronocoulometry showed the sudden increase of the Tl coverage to 0.79 monolayer at this potential.[22] By way of contrast, the dotted line in Figure 1b indicates the control experiment without Tl^+, where the peroxide reduction commences at a quite negative potential. This proves that the presence of Tl is responsible for the catalytic activity toward the H_2O_2 reduction. The Tl provides a 6.5-fold enhancement in peroxide reduction at −0.33 V.

The potential at which the electroreduction current drops suddenly (−0.37 V) occurs some 190 mV more negative of the potential of peak C in the Tl upd voltammetry. Initially, this result was surprising, as the phase change in the Tl adlayer is thought to correspond to peak C and the change in electroreduction behavior should be synchronous with this peak. An overpotential of this kind was observed in the Bi upd system, as well.[28] There are two possible sources of this overpotential. First, the magnitude of the catalytic current is so high that an effect due to the solution *iR* drop might be manifested. The solution resistance R_s is measured by impedance techniques to be ca. 20 Ω for our electrochemical cell, and the catalytic current is as large as 8.9 mA at its maximum. The overpotential due to the *iR* drop is then estimated to be 20 Ω × 8.9 mA = 178 mV, which is close to the measured value. Furthermore, in control experiments made using 0.5 M $HClO_4$, in which R_s is ca. 5 times lower than that in 0.1 M $HClO_4$, the overpotential is reduced to 35 mV, which is about 5 times smaller than the 190 mV obtained in 0.1 M $HClO_4$.

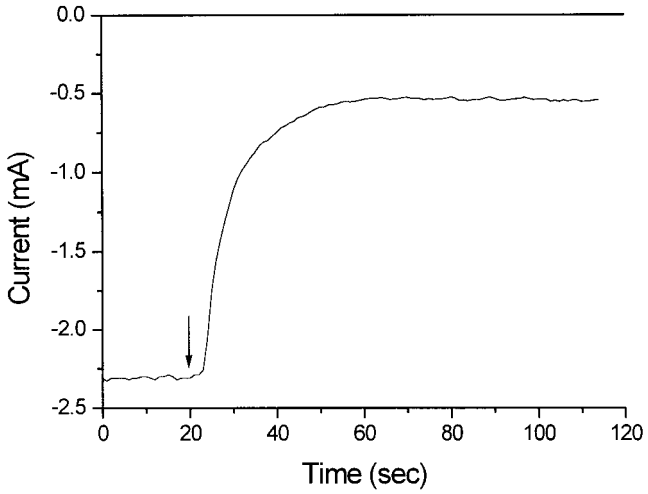

Figure 2. Chronoamperometric measurement of catalysis inhibition by 97 μM EtSH at a electrode potential of 0.04 V on the Au(111) single-crystal electrode rotating at 400 rpm in Ar-purged solution consisting of 10 mM H_2O_2, 5 mM $TlNO_3$, and 0.1 M $HClO_4$. A small volume of EtSH is injected into the slowly stirred solution at the time indicated by the arrow.

The second possibility for the origin of the overpotential might derive from the high flux of H_2O_2 impinging onto the Tl upd adlayer in the rotating disk electrode. This high flux might affect the potential at which the structural change occurs in the Tl adlayer. In the SXS measurement of the Tl full adlayer in acid solution, it was recognized that the presence of O_2 makes the adlayer structure more disordered.[21] However, the same effect should be manifested with the higher acid concentration. Thus, we favor the first explanation for the origin of the overpotential.

The inset to Figure 1b plots the maximum catalytic current with respect to the square root of the rotation speed. At slower rotation speeds, the plot exhibits a linear relation, as the Levich equation predicts.[33] However, when the rotation speed exceeds 2500 rpm, the catalytic activity of the Tl upd toward the H_2O_2 reduction begins to saturate. The maximum reaction rate is estimated to be 6.2×10^{16} s^{-1} cm^{-2} for the H_2O_2 reduction by the Tl upd on Au(111). As a reference, the Bi upd on Au(111) in the same experimental conditions gave the value of 9.1×10^{15} s^{-1} cm^{-2}.[28] The nearly order of magnitude difference in rates might relate to the different potentials of maximum current with the Tl maximum occurring at a potential 660 mV more negative than that of Bi.

3.2. Catalysis Inhibition by Poisoning. To examine further the catalytic electroreduction of peroxide by the Tl upd adlayer, we interrogated this system by deliberately introducing ethanethiol (EtSH) as a poison.[34] Figure 2 shows the temporal change of peroxide reduction activity in the Tl upd on the Au(111) system following the introduction of EtSH. Holding the electrode potential at 0.04 V gives rise to a steady-state current associated with the reduction of H_2O_2 of 2.3 mA as shown in the first 20 s plotted in Figure 2. At this potential a small volume of EtSH is injected at the moment indicated by the arrow into the slowly stirred electrolyte solution. The electrolyte solution becomes homogeneous within 5 s, with [EtSH] = 97 μM. The volume of the injected EtSH solution is less than 1% of the volume of the original electrolyte, so variations in $[H_2O_2]$, $[TlNO_3]$, and $[HClO_4]$ can be ignored.

(33) Bard, A. J.; Faulkner, L. R. *Electrochemical Methods*; John Wiley and Sons: New York, 1980.

(34) We are currently working on poisoning Tl upd with other molecules than EtSH. SCN^- also significantly inhibits the catalytic activity of Tl upd, which coincides with the Bi upd case.

Upon injection of EtSH, the peroxide electroreduction current decreases exponentially. As expected, higher EtSH concentrations give rise to more rapid current decreases. However, note that the catalytic current does not completely vanish to zero but rather that a substantial amount of residual catalytic current remains at equilibrium. The existence of this residual current is unexpected, since thiols are known to associate strongly with many metal surfaces and provide full coverage monolayers even when developed from low concentration solutions.[35] In the case of peroxide electroreduction catalyzed by Bi, for example, we found that equivalent EtSH concentrations were sufficient to completely quench catalytic activity.[28] The temporal change in current and the residue of the catalytic activity in the presence of EtSH have direct relevance to the kinetics and the thermodynamics of EtSH adsorption onto Tl upd, as will be described in detail.

To quantitatively analyze the inhibition of the catalytic activity of the Tl upd by EtSH, the RDE $I-t$ response in Figure 2 is fitted to the following formula

$$I = \Delta I \exp(-k_{app}t) + I_\infty \quad (3)$$

where ΔI is the current change after poison introduction ($=I_0 - I_\infty$, where I_0 is the initial catalytic current), k_{app} the apparent rate constant of inhibition, and I_∞ the residual catalytic current. In first-order Langmuir adsorption kinetics,[36] the temporal change of the surface coverage, θ, of an adsorbate is described as

$$\theta = K'[1 - \exp(-(k_a C + k_d)t)] \quad (4)$$

where k_a and k_d are the rate constants of adsorption and desorption, respectively, $K' = C/(C + (k_d/k_a))$, and C is the concentration of the adsorbate. In catalysis inhibition by EtSH, we assume that the residual catalytic current is proportional to unoccupied active sites

$$I/I_0 = 1 - \theta' \quad (5)$$

where θ' is the fractional coverage of EtSH on the active sites in the Tl upd adlayer on Au(111). Note that EtSH adsorption on nonactive sites would not inhibit the catalytic current and thus has no contribution to θ'.

Taking the active sites in the Tl upd adlayer as the only binding sites ($\theta = \theta'$), we obtain from eqs 4 and 5

$$I/I_0 = (1 - K') + K' \exp[-(k_a C + k_d)t] \quad (6)$$

Comparing eqs 3 and 6, the measured apparent rate constant k_{app} is related to the rate constants of adsorption and desorption as

$$k_{app} = k_a C + k_d \quad (7)$$

The catalysis inhibition experiment in Figure 2 is repeated with different [EtSH] to determine k_a and k_d. In Figure 3, the values of k_{app} measured at the various [EtSH] are plotted. Equation 7 predicts the linear relation if the adsorption process follows the first-order Langmuir adsorption kinetics. Although EtSH adsorption onto the Tl upd seems to deviate from the first-order Langmuir adsorption kinetics at the higher [EtSH], the linear region at the lower [EtSH] in Figure 3 is least-squares fitted to estimate the rate constant of adsorption k_a, which is

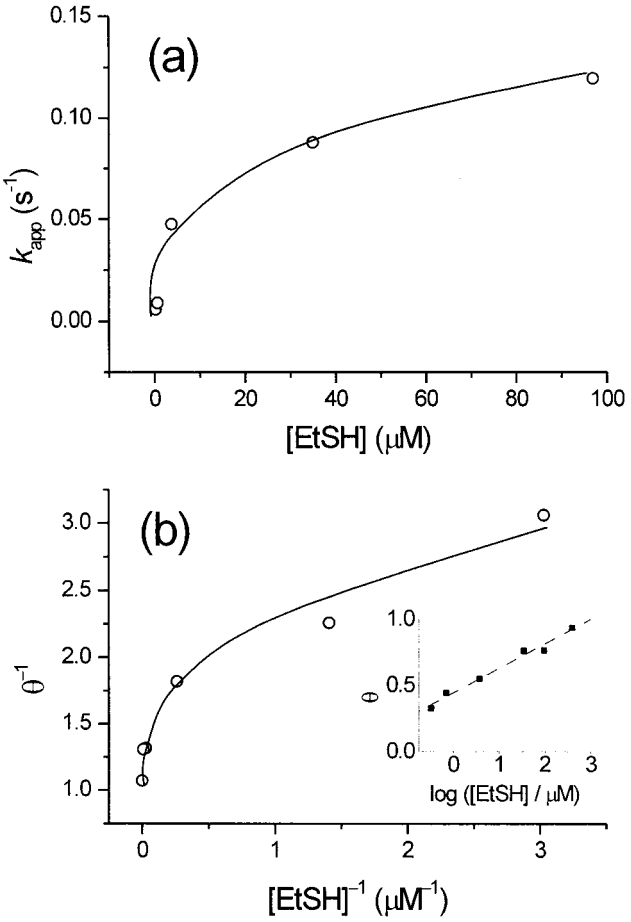

Figure 3. (a) Dependence of the apparent rate constant k_{app}, obtained by fitting the exponential decay in Figure 2, on [EtSH]. The line is to guide the eyes. (b) Dependence of the inverse of the surface coverage ($1/\theta$), obtained from the residual catalytic current in Figure 2, on 1/[EtSH]. The line is to guide the eyes. Inset: a plot of θ vs log [EtSH] (the Tempkin isotherm). The dotted line is a least-squares fit to the data.

determined to be 1.2×10^4 s^{-1} M^{-1}. For comparison, the adsorption of octadecanethiol in organic solvents onto Au proceeded with k_a of ca. 2×10^3 s^{-1} M^{-1}.[36] Also, in our previous work,[28] the adsorption of SCN^- onto the (2×2) Bi upd on Au(111) gave k_a of 1.1×10^3 s^{-1} M^{-1}. The asymptotic value as [EtSH] diminishes, which corresponds to the rate constant of desorption k_d, converges to zero within the experimental limit. This indicates that the desorption process of EtSH from the Tl upd is quite slow and can be ignored. Note that, for the adsorption process of octadecanethiol on Au, the values of k_d have significant values on the order of 0.3 s^{-1}.[36]

The residual current I_∞ in Figure 3b can be used to determine the equilibrium surface coverage θ_∞ of EtSH on the active site by

$$\theta_\infty = 1 - (I_\infty/I_0) \quad (8)$$

According to the simple Langmuir isotherm model,[37] θ_∞ relates to the concentration of the adsorbate, C, as

$$\theta_\infty = CK/(1 + CK) \quad (9)$$

or

$$\theta_\infty - 1 = 1 + (CK)^{-1} \quad (10)$$

where K is the equilibrium constant of adsorption.

(35) Dubois, L. H.; Nuzzo, R. G. *Annu. Rev. Phys. Chem.* **1992**, *43*, 437−463.

(36) Karpovich, D. S.; Blanchard, G. J. *Langmuir* **1994**, *10*, 3315−3322.

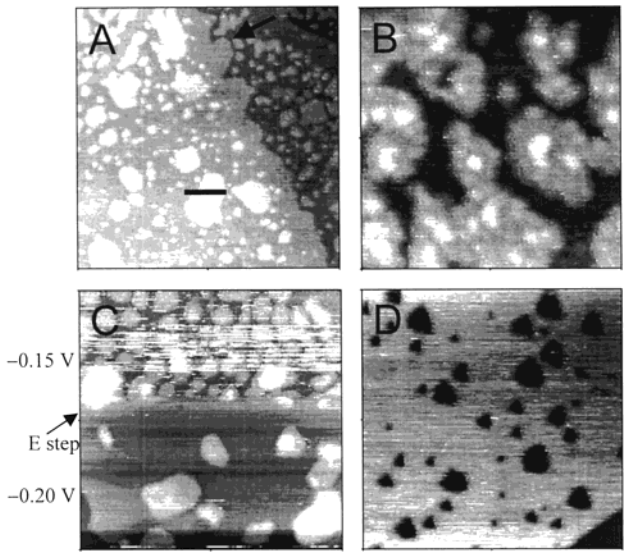

Figure 4. STM images in air-saturated solution consisting of 5 mM $TlNO_3$ and 0.1 M $HClO_4$ on Au(111). (a) 130 nm × 130 nm image of Tl islands on Au(111) terrace at $E = -0.03$ V. $I_{tip} = 2$ nA; $E_{bias} = 500$ mV. The profile along the ca. 20-nm line marked in the image is shown in Figure 5c. (b) 51 nm × 51 nm image of the second Tl adlayer deposition at $E = -0.08$ V; $I_{tip} = 2$ nA; $E_{bias} = 700$ mV. (c) 199 nm × 199 nm image of the Tl full adlayer formation. E step from −0.15 to −0.20 V; $I_{tip} = 2$ nA; $E_{bias} = 1200$ mV. (d) 90 nm × 90 nm image of the vacancy islands on Au(111) terrace after several potential cycles. $E = 0.72$ V; $I_{tip} = 2$ nA; $E_{bias} = 200$ mV.

In Figure 3b, values of θ_∞^{-1} are plotted against $[EtSH]^{-1}$. As eq 10 predicts, θ_∞^{-1} converges to 1 at the y intercept. This means that the catalytic activity of the Tl upd is almost completely inhibited by high concentrations of EtSH. The plot shown in Figure 3b deviates from the linearity predicted by the simple Langmuir isotherm model given in eq 10. The inset to Figure 3b shows a plot of θ vs log [EtSH] (the Tempkin isotherm), which seems to show better linearity, though experimental error makes unambiguous assignment of the EtSH adsorption behavior to a specific isotherm problematic. The linear region at the lower [EtSH] in Figure 3b is least-squares fitted to obtain an estimate value of the equilibrium constant K, which is determined to be 2.2×10^6 M^{-1}. K has a direct relation to ΔG_a, the free energy of adsorption, through

$$\Delta G_a = -RT \ln K \qquad (11)$$

where R is the gas constant and T the temperature. From the value of K measured from the isotherm, the ΔG_a for the adsorption of EtSH onto the Tl upd on Au(111) is determined to be about −8.6 kcal/mol. For the adsorption of octadecanethiol on Au in organic solvents, the values of ΔG_a lie between −4.4 and −5.6 kcal/mol.[36] Thus, both the kinetic and thermodyamic treatments indicate that EtSH associates more strongly with the active site of peroxide reduction in the Tl upd adlayer than does octadecanethiol with the bare Au surface.

3.3. Imaging of Tl upd on Au(111). To obtain atomic-scale structural information about the electrocatalyst surface, the Tl-modified Au(111) electrode was imaged by in situ STM. In Figure 4 are shown a series of STM images of Au(111) electrodes at various potentials in a solution containing 5 mM $TlNO_3$ and 0.1 M $HClO_4$. At potentials positive of 0.9 V, the STM image exhibits the typical Au(111) terraces and steps. As the potential becomes more negative, small islands begin to appear on Au(111) terraces as shown in Figure 4a obtained at a potential of −0.03 V. At this potential, there is considerable current associated with O_2 reduction occurring during imaging because the STM cell is not purged of O_2. This implies that the Tl structures observed are the actual structures present during electrocatalysis rather than the ones deprived of O_2 reactant.

As the potential is moved to more negative values, the number and size of the islands become greater and larger, respectively. Figure 4A also shows that the initial stages of Tl upd is manifested not only as island growth but also as growth laterally off of the Au(111) terrace, marked with an arrow in Figure 4A, as these edges grow in extent. Preferential adsorption of the upd metal on the Au(111) step edge was previously reported for Tl upd on Ag(111)[12] and Pb upd both on Ag(111)[13] and on Au(111).[14−16] The island features on the Au(111) terrace in Figure 4a are assigned to the Tl adlayer, because the islands are not observed in the absence of Tl^+. The height of the Tl islands is measured to be 0.24 ± 0.03 nm, which is so close to the that of a monatomic Au(111) step (0.235 nm) that distinguishing between Tl islands and Au(111) steps by height alone is not possible. For reference, SXS measurements of the Tl−Au interlayer spacing give a value of 0.225 nm in neutral solution[38] and 0.266 nm for the close-packed full adlayer in alkaline solution.[20] The height of the Tl islands above the Au(111) terrace is unchanged regardless of the electrode potential, which is consistent with the results from the X-ray diffraction of the Tl upd in neutral solution.[38] At potentials close to the peak C in Figure 1a, a second Tl adlayer is observed to deposit (Figure 4b) on top of the islands. The height of the second adlayer from the first adlayer is measured to be 0.22 ± 0.06 nm, which is the same as that of the first Tl adlayer. We note that second adlayer deposition in the underpotential region is rare and has only been observed for Tl upd on Ag(111)[39] and on Ag(100).[40]

Figure 4c shows the STM image obtained during a stepwise change in the electrode potential. In the upper part of the image, the electrode potential is −0.15 V, where the Tl islands are observed on Au(111) terraces. While acquiring the image, the potential is stepped to −0.20 V, a potential which is just after peak C in the voltammetry. The image shows that the Tl islands in the upper part of the image are transformed during the potential step to a Tl full adlayer. Note that the second Tl adlayer, the height of which is measured to be 0.24 ± 0.04 nm, is still present even after the Tl full adlayer formation, and in some cases even a third Tl adlayer is observed.

SXS measurement of the Tl full adlayer in the absence of O_2 revealed a rotated hexagonal structure.[21] However, in the presence of O_2, the X-ray scattering intensity is significantly reduced and the peak width increased, which indicates that the O_2 interaction with the Tl upd causes the Tl full adlayer to become laterally disordered. This observation explains the difficulty in resolving the atoms in the Tl full adlayer by using STM, in air-saturated solution. The SXS result may also explain the lack of resolution obtained for Tl in the island structures, as well.

When the potential is stepped back to more positive potentials, the Tl full adlayer transforms back to the island

(37) Adamson, A. W. *Physical Chemistry of Surfaces*, 5th ed.; Wiley-Interscience: New York, 1990.

(38) Chabala, E. D.; Harji, B. H.; Rayment, T.; Archer, M. D. *Langmuir* **1992**, *8*, 2028−2033.

(39) Toney, M. F.; Gordon, J. G.; Samant, M. G.; Borges, G. L.; Melroy, O. R. *Phys. Rev. B* **1992**, *45*, 9362−9374.

(40) Wang, J. X.; Adzic, R. R.; Magnussen, O. M.; Ocko, B. M. *Surf. Sci.* **1995**, *344*, 111−121.

structure. As the potential becomes more positive, the size and number of Tl islands becomes smaller. However, remnants of Tl islands are still observed even at a potential as positive as 1.2 V, where Tl^+ is oxidized to Tl^{3+}.

Figure 4d is an STM image of the Au(111) terrace after the Tl full adlayer is deposited and stripped several times by the potential cycling. A larger population of vacancy islands are observed with the depth of 0.25 ± 0.02 nm, which corresponds well to the Au(111) step height (0.235 nm). Vacancy island formation in the underpotential region has been previously reported for Pb upd on Au(111)[17] and is interpreted to arise from the adlayer−substrate alloying. We also note the triangular shape and alignment of the vacancy islands, which indicates anisotropic etching of the Au(111) terrace by desorption of the alloyed Tl upd adlayer.

3.4. Imaging of Tl upd on Au(111) Poisoned with EtSH. To visualize the catalytically active sites in the Tl upd island structure on Au(111), the system was investigated following the introduction of EtSH. After observing the Tl islands on Au(111) by STM at the potential just positive of peak C of Figure 1a in 5 mM $TlNO_3$ and 0.1 M $HClO_4$, a small amount of EtSH was injected into the STM cell, with [EtSH] = 0.2 mM. At −0.2 V, EtSH is reductively desorbed from the bare Au(111) electrode surface.[41] This desorption prevents EtSH from adsorbing on the Au terraces and makes analysis of STM image much simpler, as will be shown below.

Figure 5a shows an STM image of Tl upd on Au(111) after EtSH injection. While the adlayer maintains the island structure, an additional feature is observed at the edges of the Tl islands. The edge decoration of the Tl island upon EtSH injection is more clearly presented in the profile in Figure 5b, which is taken along the line marked in Figure 5a. For comparison, the line profile of the Tl island on Au(111) in Figure 4a without EtSH is shown in Figure 5c. In Figure 5b, the height of the terrace T_1 is measured to be 0.25 ± 0.04 nm above the bare Au(111), which is the same as that of the Tl island without EtSH in Figure 5c. On the basis of this height similarity, we assign the terrace T_1 to the Tl island which was present before EtSH addition.

The additional terrace T_2, which develops in the presence of EtSH, exhibits a height of 0.16 ± 0.02 nm above the Au(111) terrace and can be clearly distinguished from the Tl island. Because the edge decoration T_2 develops only in the presence of EtSH and because the height of the terrace T_2 is too small to result from Tl or Au, we associate the terrace T_2 with adsorption of EtSH at the Tl island edges. In a STM study of thiol adsorption on Au(111) in ultrahigh vacuum,[42] $HS(CH_2)_6OH$ exhibits apparent heights of 0.08 nm relative to the Au surface when the alkyl chains lie flat on the surface and 0.18 nm—close to that observed here—when they align with the surface normal. The alkyl chain contributes negligibly to the apparent height measured by STM.

The T_2 region extends from the Tl island edge by some 10 nm, indicating the presence of more than a single row of EtSH. The EtSH appears to agglomerate at the step edge of the Tl island extending a limited distance. As indicated by the straight arrow in Figure 5a, the EtSH terraces are easily linked between the neighboring Tl islands, which might be encouraged by van der Waals interactions between the alkyl chains of EtSH. Since EtSH does not adsorb on bare Au(111) at the potentials at which these images were obtained, the presence of this material

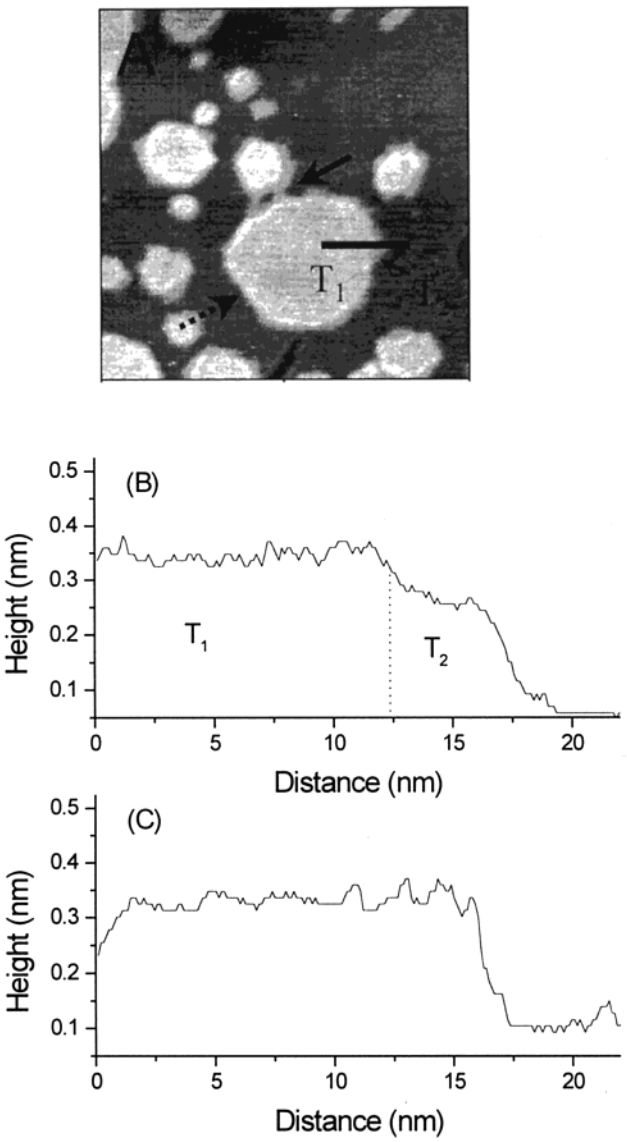

Figure 5. (a) 102 nm × 102 nm STM image of Tl islands in the presence of 0.2 mM EtSH at the potential just positive of peak C in Figure 1a (about −0.2 V). I_{tip} = 1 nA; E_{bias} = 800 mV. (b) Line profile of the Tl island decorated with EtSH along the line marked in Figure 5a. (c) Line profile of the Tl island without EtSH, which is taken along the line marked in Figure 4a. The *x* axis is reversed for easy comparison.

below the Tl step edge suggests a different electronic structure for the Au atoms next to the Tl islands.

As indicated by the EtSH adsorption isotherm in Figure 3b, the EtSH coverage on the active sites in the Tl upd system depends on [EtSH]. Approximately 86% of these active sites are blocked with [EtSH] = 0.2 mM. The STM image shows that the edge sites of the Tl islands are not uniformly decorated with the EtSH terrace, but rather evince Tl step edge areas which are not covered with EtSH, as indicated by the dashed arrow in Figure 5a. As [EtSH] increases, the EtSH terrace tends to cover the entire edge area of the Tl island. Alternatively, observation of the EtSH terrace becomes difficult when [EtSH] is lower than 0.1 mM.

The extent of the EtSH terrace feature also depends on the electrode potential. When the potential is swept to −0.25 V, the EtSH terrace is laterally enlarged. Alternatively, when the potential is positive of −0.07 V, where EtSH adsorbs to the Au(111) terrace, the EtSH terrace feature disappears and a myriad of vacancy islands are observed to cover both the Au and Tl terraces. This

(41) Hagenstrom, H.; Schneeweiss, M. A.; Kolb, D. M. *Langmuir* **1999**, *15*, 2435−2443.
(42) Poirier, G. E.; Pylant, E. D. *Science* **1996**, *272*, 1145−1148.

observation indicates that EtSH binds not only at the Tl island edges but to the whole surface at this positive potential. We also note that when the potential is swept back to −0.2 V, the STM image again shows the EtSH terrace at the Tl island edge sites. This implies that EtSH terrace formation is a reversible process.

4. Discussion

Compared with other upd systems, Tl upd on Au(111) in the acid electrochemical environment exhibits unique features and its structure verified in this work has important consequence to the mechanism of electrocatalysis. Also we will discuss the poisoning of the Tl upd by EtSH in terms of the active site of catalysis.

4.1. Structure of the Tl upd. There are three different potential regions for the Tl upd system in which different structures are observed. At positive potentials, just negative of that required to oxidize Tl^+, STM images reveal only the bare Au(111) terrace. As the potential becomes more negative—and cathodic current due to the O_2 reduction begins to increase—the Tl adlayer grows at the Au(111) step edge and a large number of Tl islands appear on the Au(111) terrace. When potential is negative of the peak C in Figure 1a, the Tl full monolayer covers the whole Au(111) surface.

These STM results are in accord with previous work using SXS to examine the Tl upd system. In particular, both techniques report that the structure of the Tl upd system at potentials negative of peak C is a full monolayer. However, in the intermediate, catalytically active potential region, the SXS measurements were unable to reveal the Tl adlayer structure, which the present STM data show to be an island structure.[21] This result suggests that either the Tl atoms in the island structure have little internal regularity or that the X-ray might be intrinsically attenuated when scattered from the nonuniform island structure.

The height of the Tl island relative to the Au(111) (0.24 nm) measured by STM is close to the Au(111) interlayer spacing (0.235 nm), although the bulk Tl interatomic distance (0.342 nm) is 17% larger than that of Au (0.292 nm). The compressed Tl−Au interlayer distance implies a strong interaction between Tl and Au atoms. This is also manifested in the rearrangement and the etching of the Au(111) terrace upon Tl deposition and stripping in Figure 4d. The height of the second Tl adlayer relative both to the first Tl island (0.24 ± 0.04 nm) and to the full Tl adlayer (0.22 ± 0.06 nm) also seems to be compressed with respect to the bulk interplanar distance of Tl. This might imply that Tl adatoms strongly interact vertically in the underpotential region.

There are two aspects of the Tl upd on the Au(111) system which are unusual relative to most upd systems. First, the deposition proceeds via an island structure. Most upd systems construct a uniform adlayer that covers the whole terrace area of the substrate. While this uniform adlayer is achieved in the most negative potential region for Tl, such is not the case positive of peak C. The only other upd system known to exhibit an island motif is Pb upd on Au(111).[14−18,24] Tl and Pb, which are neighbors in the periodic table, resemble each other both in the upd adlayer structure and in the cyclic voltammogram.[22] That islands exist in both of these upd systems speaks to the relatively strong associative adatom−adatom interaction. In many other upd systems, the presence of open partial monolayers is interpreted as arising from the presence of repulsive forces derived from coadsorbed anions. In Tl upd on Au(111), chronocoulometric measurements showed that a substantial amount of hydroxide is coadsorbed on the upd adlayer even in the acid media.[22] This coadsorbed hydroxide must play an important role to stabilize the Tl island structure in which Tl atoms are not fully discharged. However, it is unclear whether the hydroxide decorates the Tl island uniformly or whether it is located exclusively at the island edges. In the alkaline environment, no island structure is reported in the Tl upd,[19] which might indicate that the higher concentration of hydroxide provides the repulsive component to disrupt the island structure and lead to the more uniform Tl adlayer structure.

The second unusual aspect of the Tl upd system is that the Tl island adsorption proceeds in a continuous manner and shows no clearly resolved voltammetric peaks. In most upd processes, the adsorption process is usually accompanied by a distinct voltammetric peak and does not proceed in a continuous fashion. The images obtained in this study—as well as the coverage derived from chronocoulometric measurements[22]—strongly suggests that continuous variation in Tl coverage on the Au surface does occur. The origin of this behavior is unclear but may result partially as a consequence of strong Tl−Tl interactions which would favor continued growth of the monolayer once nucleation has occurred.

4.2. Reactivity. While the rate of H_2O_2 reduction is very slow on the bare Au(111) electrode (Figure 1b), the presence of upd Tl greatly enhances the reactivity of the Au(111) electrode toward the H_2O_2 reduction. The Tl upd begins to catalyze the H_2O_2 reduction at the potential as positive as 0.5 V and the catalytic activity monotonically increases over a wide potential range until the electrode loses activity at −0.37 V due to the structural transformation from Tl islands to a uniform (1×1) Tl adlattice. The potential range in which the catalytic current increases is quite broad relative to Bi upd on Au(111) in which the formation of (2×2) Bi adlayer occurs at a specific potential and the catalytic current rises only within a small potential range.[28] The wide potential range of catalytic activity in the Tl upd evidently comes from the continuous evolution of the Tl island structure.

It is interesting to compare the relative catalytic activity of the Tl upd and the Bi upd systems toward peroxide electroreduction. The maximum catalytic activity for Tl upd occurs at the potential about 0.66 V more negative than for Bi upd.[28] From the simple relation between the overpotential ΔE and the current I,[33] i.e., $I \propto \exp(\alpha nF\Delta E/RT)$, where α is the transfer coefficient, n the number of electrons per molecule, F the faradaic constant, R the gas constant, and T the temperature, the catalytic current would be multiplied by a factor of ca. 10^{11} when $\Delta E = 0.66$ V, $\alpha = 0.5$, and $n = 2$. However, the maximum rate of H_2O_2 reduction by the Tl upd is only about 7 times larger than that by the Bi upd. By comparing the coulometric-derived coverage data with that measured for the reactivity, we calculate that the limiting rate of electroreduction is ca. 77 per adsorbed Tl adatom per second while the corresponding rate in the 25% coverage (2×2) Bi upd system is ca. 26 per Bi adatom per second. This comparison lowers the difference between the two upd systems even further. At the potential where the Bi upd system is active, the electroreduction rate in the Tl system is very small.

Although the comparison between the two upd systems might not be as straightforward as described above, this comparison does gives us some insight into the reactivity of the electrocatalyst. The comparatively low intrinsic catalytic activity of the Tl upd system may indicate that the density of the active sites in the Tl upd is much lower than that in the Bi upd. In the Bi upd on Au(111) system, the (2×2) Bi adlayer covers the whole Au(111) terraces

and each unit cell can act as the active site. However, in the Tl upd on Au(111), a substantial area of uncovered Au surface is exposed, thus leading to a lower density of the active sites. Furthermore, if the catalysis occurs only at the edge site of the Tl island, as will be discussed below, the density of the active sites would be much lower than when the whole Tl island acts as the active site, resulting in the much lower intrinsic catalytic activity of the Tl upd system.

4.3. Poisoning Catalysis by Tl upd. Judging from the free energy of adsorption ΔG_a, the association of EtSH to the active site of peroxide electroreduction in the Tl upd system is ca. 4 kcal/mol stronger than that on the bare Au. This energetic result explains the fact of EtSH adsorption even at the quite negative potential where EtSH is expected to reductively desorb from the Au(111). Since the STM images show that EtSH associates with the Tl upd system only at the island step edges, this result suggests that the electronic structure of the island edges is different from that of either the Tl present in the interior of the islands or the bare Au(111) terrace.

The images also show that association of EtSH to the Tl upd/Au(111) system is not exclusively at the step edges, as the terrace associated with the molecule extends some 10 nm away from the Tl island. The EtSH structures appear to exhibit a tendency to coalesce with each other, as shown in Figure 5A. This suggests that van der Waals interactions among the alkyl chains of EtSH are important in the interaction of the molecule with the surface, a result not unanticipated from other studies of thiols adsorbed on Au surfaces.[35] We note that the EtSH adsorption isotherm in Figure 3b seems to deviate from the simple Langmuir isotherm and to better fit the Temkin isotherm, an isotherm that explicitly considers adsorbate−adsorbate interactions.

4.4. Structure−Reactivity Correlation. The existence of the Tl island structure at the potential of catalytic activity indicates that the Tl island is where O_2 actually binds and reacts in the catalytic reduction. There are two candidates for the active site in the Tl island: the terrace area and the edge site of the Tl island. The experimental results suggest strongly that the edge site is the active site. First, the Tl full monolayer shows no catalytic activity. This implies that the availability of Au as well as of Tl site is essential for the catalysis to occur and the edge site in the Tl island structure is where both Tl and Au are accessible. Second, the preferential adsorption of EtSH at the edge site of the Tl islands and the accompanied inhibition of the catalytic activity shows that the edge site is energetically different compared to other sites and the origin of the catalytic activity.

What is the possible mechanism of electroreduction activity? There are several possibilities here related to both heterogeneous and homogeneous mechanisms. In the heterogeneous mechanisms, the dioxygen or peroxide could associate with the Tl, the Au, or both at the Tl island step edge. The special electronic and/or geometric properties of the atoms in this location could then be associated with the reduction activity. Some insight into the appropriate choice is given by the location of inhibition by EtSH. EtSH associates with Au at the Tl island step edges at potentials considerably more negative than possible on the bare Au(111) terrace giving rise to a 4 kcal/mol stabilization at the island edges relative to the Au terrace. This result suggests that a consequence of Tl island formation is to remove electron density from the Au atoms near the Tl islands. In other words, the reduction of Tl^+ during the upd process leaves the neighboring Au atoms somewhat electron deficient. This electropositive site could be the location of peroxide or dioxygen association with the electrode surface. More definitive vibrational spectroscopic measurements will be required to evaluate this possibility.

Second, the Tl at the island step edges could be associated with a homogeneous redox mechanism. In SXS measurements made on TlBr overlayers on Au(111) in acid solution, Adzic and Wang observed that Tl coverage on this surface is significantly reduced during catalytic O_2 reduction. These authors proposed that Tl oxidation to reduce dioxygen followed by rereduction/redeposition of Tl onto the Au surface is the origin of the catalysis.[27] The corresponding process in our system would involve oxidation of Tl adatoms at Tl island step edges which would then be somehow stabilized by the inhibiting EtSH. If this mechanism were operative in the Tl island system, we would expect to observe evidence of fluxional behavior at the Tl island step edges in the absence of EtSH. This fluxional behavior should be manifested either as long-term changes in the island shape and/or the presence of "frizzies" which are indeterminacy in step edge position observed during STM scanning resulting from movement of adatoms along and away from the step edge. "Frizzies" have been observed on Ag surfaces in aqueous solution under potential control.[43] Neither of these behaviors is observed for the Tl upd islands, even during the electrocatalytic event. Finally, we note that the environment under the STM tip might be oxygen deficient relative to areas not being scanned. However, we anticipate that at long times enough oxygen will have diffused under the tip to produce the changes expected above. These observations lead us to favor heterogeneous mechanisms over putative homogeneous ones.

Why should the Tl island structure behave in a manner different from TlBr? The Tl upd and the TlBr system have some fundamental differences. The simple Tl adlayer exhibits the characteristic island structure, while TlBr evinces a uniform adlayer on Au(111). From previous work we know that OH^- is coadsorbed in the Tl island structure.[22] Also, the coadsorbed OH^-, the role of which in the O_2 reduction is well recognized,[26] maintains the simple Tl adlayer. On the contrary, OH^- is likely to be replaced by the strongly adsorbing Br^- in the TlBr adlayer.

5. Conclusion

We performed electrochemical and STM measurements in order to establish a structure−reactivity correlation for electrocatalytic O_2 reduction by the Tl upd on Au(111) in acid. STM images reveal that an island structure composed of Tl adatoms exists on Au(111) terraces at the potential of catalytic activity. Introduction of EtSH leads to significant inhibition of electroreduction activity. STM images show that EtSH adsorbs exclusively on Au at the edge sites of the Tl island. This EtSH adsorption occurs at the edges of the Tl upd islands more strongly than on bare Au(111), suggesting that the Au atoms near the Tl upd islands are more electropositive than the corresponding Au atoms on the bare Au(111) terrace. These results strongly favor a heterogeneous mechanism for dioxygen electroreduction involving dioxygen association at edge sites on the Tl islands.

Acknowledgment. This work was supported in part by the Brain Korea 21 Project in 2000 and by the Korea Science and Engineering Foundation through the MICROS center at KAIST, Korea. A.A.G. acknowledges the NSF (CHE-9820828) for partial support of this research.

LA010297U

(43) Giesen, M.; Randler, R.; Baier, S.; Ibach, H.; Kolb, D. M. *Electrochim. Acta* **1999**, *45*, 527−536.